ARTICLES

Inorganic Salt Hydrates as Cryoporometric Probe Materials to Obtain Pore Size Distribution

D. Vargas-Florencia, O. Petrov, and I. Furó*

Division of Physical Chemistry and Industrial NMR Center, Department of Chemistry, Royal Institute of Technology, SE-10044 Stockholm, Sweden

Received: October 16, 2005; In Final Form: December 19, 2005

The depression of the melting temperature of $Zn(NO_3)_2 \cdot 6H_2O$ was used to obtain the pore size distributions in controlled pore glasses. Measured by ^1H NMR, the average value of the temperature depression ΔT and the known average pore size yield $K = \Delta T \cdot d \approx 116$ K·nm as the material-dependent factor for $Zn(NO_3)_2 \cdot 6H_2O$ in the Gibbs-Thompson equation. The melting temperature is close to room temperature. Hence, this salt hydrate and some related other ones are better materials than water ($K \approx 50$ K·nm) for cryoporometric studies of systems with hydrophilic pores. The data also provide 46 mN/m for the solid−liquid surface tension of this salt hydrate.

Introduction

Cryoporometry, either by differential scanning calorimetry (DSC)[1−3] or by nuclear magnetic resonance (NMR)[4−8] as a detection tool, has recently found widespread application in measuring pore sizes and pore size distributions in various materials. The technique is based on the depression of the freezing and melting points of confined substances.[9] Relative to the bulk, the melting point depression of a confined solid is customarily described (here, for a cylindrical pore[10,11]) by the Gibbs-Thompson equation

$$\Delta T = \frac{2\gamma_{sl}\nu T_0}{\Delta H_f d} \tag{1}$$

where ΔH_f is the bulk enthalpy of fusion, T_0 the bulk melting point, ν the molar volume, and γ_{sl} is the surface tension of the liquid−solid interface. We note that the freezing and melting temperatures are different for confined materials and so are the equations that describe them. The validity of eq 1 has been verified[11] by applying it to the melting of well-characterized materials, such as water, in well-characterized porous systems, such as controlled pore glasses. Assuming that all parameters in eq 1 are independent of pore size and temperature,[12] eq 1 reduces to

$$\Delta T = \frac{K}{d} \tag{2}$$

where K is a material property. Hence, by measuring ΔT and its spread within a particular porous system, one can obtain the average pore size and the pore size distribution. The value of K for a specific compound is a direct indicator of its sensitivity to pore diameter; i.e., the larger the value of K, the larger the melting point depression.

Conventionally, pore size distributions have been obtained by organic liquids such as cyclohexane or water as probe molecules. Of these, particular organic liquids[1] are chosen because they have a larger K value than that of water (∼50 K·nm). Moreover, water expands upon freezing and, hence, freezing of the intrapore water may damage the investigated porous network. On the other hand, organic liquids may not be imbibed into pores with hydrophilic surfaces.

Irrespective of the probe material, the actual experiment involves the detection of melting (typically) or freezing (less often since it is also affected by supercooling) of the particular probe material that, in its liquid form, has been imbibed into the pores. In DSC cryoporometry (also called thermoporometry), this is done calorimetrically. In NMR cryoporometry, one explores the distinct difference in molecular dynamics and therefore in transverse relaxation times between liquids and solids which typically causes the spin−echo NMR signal to vanish in solids but not in liquids.

In this work we introduce a new class of cryoporometric probe materials: stoichiometric hydrates of inorganic salts. In particular, ^1H NMR cryoporometric data will be presented below for zinc nitrate hexahydrate within a controlled porous glass (CPG). To our knowledge, no inorganic compounds have been used before in cryoporometry.

Experimental Section

Uncoated controlled porous glasses (CPG) from Millipore Corp. were used; experiments were performed in a material with a mean pore diameter of 31.3 nm, a specific surface area of 66.7 m^2/g, a surface-to-volume ratio of 66.7×10^6/m, a specific pore volume of 1.00×10^{-6} m^3/g, and the relative width of pore size distribution of ca. 6% (data as supplied by the manufacturer, 90% of pores within this range). Two other

* Corresponding author. E-mail: ifuro@physchem.kth.se. Tel: +46 8 7908592. Fax: +46 8 7908207.

10.1021/jp055915k CCC: $33.50
Published on Web 02/08/2006

TABLE 1: Material Properties of Some Inorganic Salt Hydrates and, for Comparison, Those of Water

substance[a]	melting point (K)	enthalpy of fusion (kJ/mol)	surface tension (mN/m) liquid−vapor	surface tension (mN/m) solid−liquid	solid density (g/cm^3)
H_2O	273.2	6.01	76	30[29]	0.92
$Zn(NO_3)_2{\cdot}6H_2O$	309.4[30]	39.91[30]	91[15]	46[b]	2.067[31]
$Ca(NO_3)_2{\cdot}4H_2O$	315.5[32]	31.05[32]	96.6[15]		1.896[33]
$CaCl_2{\cdot}6H_2O$	302.7[34]	43.40[34]		49[b]	1.71[31]
$Mn(NO_3)_2{\cdot}6H_2O$	298[35]	40.26[35]	95.1[15]		1.82[33]
$Fe(NO_3)_2{\cdot}9H_2O$	321.7[33]	76.99[33]	77.5[15]		1.684[33]

[a] $X(NO_3)_2{\cdot}6H_2O$ with X = Mn, Co, or Fe are paramagnetic liquids. [b] This work.

glasses with 15.6 and 23.7 nm mean pore diameters were also investigated. These porous glasses have a random tube network appearance that locally might be well-represented as cylindrical.[13] Zinc nitrate hexahydrate (≥99%) was used as obtained from Fluka; see its material properties in Table 1. Crystals of $Zn(NO_3)_2{\cdot}6H_2O$ melt at around 40 °C as observed visually in an oven and yield a homogeneous liquid phase. Further heating of the solution was avoided to prevent evaporation of water.

Due to supercooling of the molten salt, it was possible to imbibe the liquid into the CPG at room temperature. However, imbibition also occurs by simply loading crystals of $Zn(NO_3)_2{\cdot}6H_2O$ over CPG grains laid at the bottom of an NMR tube and thereafter placing the tube into a 40 °C oven. Obviously, the melt wets the pore surface (one contribution is hydrogen bonding to hydroxyl groups of the porous matrix). The samples prepared for the present study all contained an excess (with respect to the estimated pore volume) of $Zn(NO_3)_2{\cdot}6H_2O$. The excess liquid that remained outside the porous glass grains provided the bulk melting temperature reference during the experiments. Moreover, this bulk phase also promotes freezing inside the pores by initiating crystals to grow from outside into the pores. Furthermore, by knowing the total amount of added materials (CPG and, in this case, the salt hydrate) and by measuring the ratio of the NMR signal intensities corresponding to the total (measured above the bulk melting point) and pore-filling (measured directly below the bulk melting point) materials, the pore volume and its distribution can be expressed in absolute instead of relative units. Hence, the unit of pore size distribution becomes cm^3 g^{-1} nm^{-1}, as shown below in Figure 3.

The ^{1}H NMR measurements were carried out on a Bruker DMX200 spectrometer with 200 MHz frequency for protons and equipped with a standard 10 mm probe. The temperature was controlled by a precision of 0.1 K by a Bruker BVT3000 temperature controller. The temperature spread within the same sample volume was estimated to about 0.3−0.4 K by ^{59}Co NMR spectroscopy of an aqueous solution of $K_3Co(CN)_6$. The magnetic properties of inorganic salt hydrates are governed by the involved transition metal ions; Zn^{2+} is diamagnetic and, hence, provides a magnetically unbroadened NMR spectrum. Note that several of the compounds listed in Table 1 contain paramagnetic ions and are therefore less suitable for cryoporometric NMR (but not for DSC) experiments.

The samples with imbibed $Zn(NO_3)_2{\cdot}6H_2O$ were first cooled to ∼250 K whereupon the added liquid froze. While the temperature was then increased in 0.1 K steps, spin−echo experiments with $90°-\tau-180°-\tau$ acquisition were carried out with $\tau = 1$ ms. Achieving equilibrium (typically 5−10 min after the temperature change) was verified by recording a persistent signal intensity. The resulting temperature-dependent intensity data are given in Figure 1; all reported intensities are spectral integrals. As verified by transverse relaxation time T_2 data measured by the conventional Carr-Purcell-Meiboom-Gill method (see Figure 2), the signal intensity $I(T)$ recorded by this echo time is proportional to the molten fraction of imbibed $Zn(NO_3)_2{\cdot}6H_2O$. T_2 of the frozen solid phase has been estimated to ∼20 μs and therefore that phase does not contribute to $I(T)$. Note that the relaxation data presented in Figure 2 correspond to a variety of liquid phases (see also discussion below).

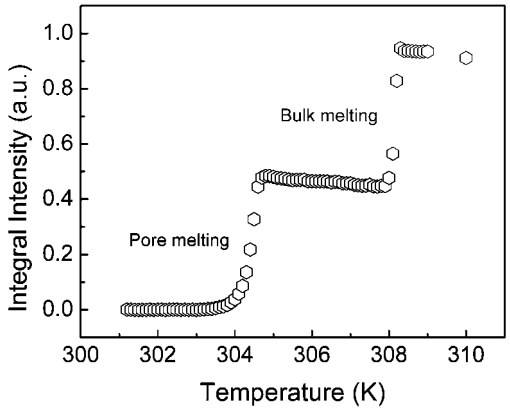

Figure 1. The temperature variation of the intensity of the ^{1}H NMR spin−echo signal $I(T)$ during melting of $Zn(NO_3)_2{\cdot}6H_2O$ in bulk and imbibed into a controlled porous glass of 31.3 nm average diameter.

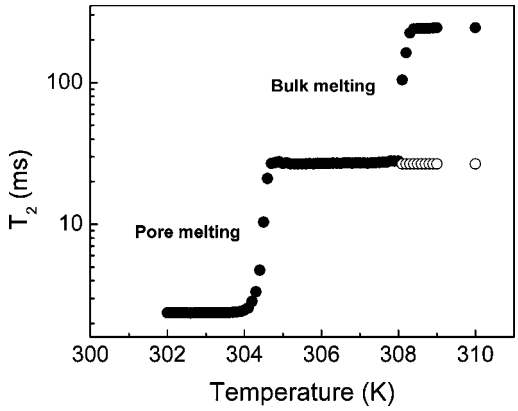

Figure 2. ^{1}H transverse relaxation time T_2 of $Zn(NO_3)_2{\cdot}6H_2O$ imbibed in a controlled pore glass with mean pore size 31.3 nm. Below the bulk melting point, single-exponential fits provided T_2. Above the bulk melting point, two-exponential fits with the bulk T_2 fixed to a value measured in separate experiments in bulk provided the T_2 of the pore liquid (empty symbols). Below pore melting, a small signal component with short T_2 arises from the nonfreezing surface layer of $Zn(NO_3)_2{\cdot}6H_2O$.

Results and Discussion

In recent years, the physicochemical properties of inorganic salt hydrates have been subject to a number of investigations due to their applicability in thermal energy storage: they have large volumetric thermal storage densities (as a consequence of high enthalpies of fusion), high thermal conductivities, but low melting points.[14] Generally, the low melting point of hydrates of inorganic salts such as carbonates, nitrates, sulfates, acetates, and halides is connected to the water of hydration that is an integral part of their crystal structure. An extensive search for the cryoporometrically promising compounds was carried out, with some representative results shown in Table 1. For compounds having the same functional group (nitrates in this case), salts that contain the same number of hydration water molecules per cation appear to have almost identical properties such as the enthalpy of fusion. Such compounds also have very

close equivalent volumes, irrespective of the charge or radius of the cation.[15] On the other hand, for the same compound the enthalpy of fusion decreases and the melting point increases upon decreasing water content (e.g., $Zn(NO_3)_2 \cdot 4H_2O$, $Zn(NO_3)_2 \cdot 2H_2O$, and $Zn(NO_3)_2 \cdot H_2O$ melt at 44.7, 55.4, and 73.9 °C, respectively[16]).

To carry out our demonstration, we selected zinc nitrate hexahydrate from a group of a few dozen possible compounds (note that very similar data, although not shown here, were also obtained for $CaCl_2 \cdot 6H_2O$; see derived surface tension in Table 1). From the point of view of NMR cryoporometry, $Zn(NO_3)_2 \cdot 6H_2O$ is an optimal material: its melting point is 308.4 K; i.e., just above room temperature, it forms a bulk homogeneous molten phase, crystallizes in a homogeneous orthorhombic structure with octahedral symmetry, and is diamagnetic (important for the NMR measurements). Both in glass[17] and in crystal[18] states, the nearest coordination shell of Zn^{2+} in $Zn(NO_3)_2 \cdot 6H_2O$ is filled with water, which displaces the NO_3^- ions onto a peripheral shell. $Zn(NO_3)_2 \cdot 6H_2O$ can rapidly adapt its crystalline structure through progressive rearrangements of the $[Zn(H_2O)_6]^{2+}$ groups. The presence of coordinative unsaturation around the transition metal (Zn^{2+}) and the corresponding coordinated water also lends this compound other applications such as in metal-dispersed catalysis[19] and in high-energy-density batteries.[20]

As shown in Figure 1, the melting transition for bulk crystals is sharp within a range of ~0.3 K that can be predominantly assigned to temperature spread within the sample volume. This is the instrumental limitation (not absolute, but dependent among other factors on the sample size) on the resolution of the obtained pore size distributions. The melting transition is much broader for the imbibed material and we assign this broadening to pore size distribution. From the 3.7 K temperature difference between the bulk melting point and the midpoint of the porous melting curve and the average pore size of 31.3 nm, we obtain the experimental value of $K = 116$ K·nm via eq 2. Hence, zinc nitrate hexahydrate is more than twice as sensitive as water in measuring porous structures. In fact, its K value is close to those of organic probe compounds[1,6,21] like benzene and cyclohexane but zinc nitrate hexahydrate is hydrophilic and therefore easier to imbibe in various hydrophilic porous materials such as ceramics, glasses, or certain rocks. The pore size distributions in Figure 3 obtained through

$$P(d) = \frac{K}{d^2}\frac{\mathrm{d}I(T)}{\mathrm{d}T} \tag{3}$$

are narrow. Their relative widths are ~9−12% (90% of pores within this range) where we corrected (by simple subtraction) for the experimental resolution given by the temperature spread; in relative units this correction factor is approximately 8%, 6%, and 4% for the samples with 31.3, 23.7, and 15.6 nm nominal pore sizes. Our widths of pore size distributions are somewhat higher than the corresponding values (~4−6%) reported by the manufacturer which may reflect the differences between the applied experimental methods; NMR cryoporometry essentially measures differences in pore volumes with a given size while mercury porosimetry estimates the sizes of pore openings.

The obtained K value can also be used to estimate the one material property involved in eq 1 that is difficult to determine by other means: the solid−liquid surface tension γ_{sl}. Since the other involved properties are known to a reasonable accuracy, 46 mN/m is obtained for γ_{sl} which is roughly half the value of the liquid−vapor surface tension γ_{lv} (see Table 1).

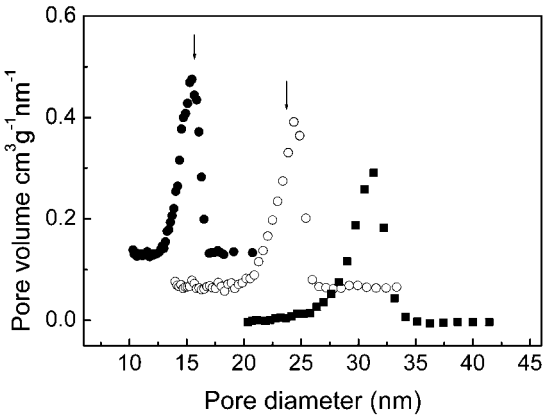

Figure 3. Pore size distributions $P(d)$ in controlled pore glasses of 15.6 nm (●), 23.7 nm (○), and 31.3 nm (■) nominal pore diameters, obtained via eq 3 from data as in Figure 1 (for the 31.3 nm CPG). The K value in eq 3 was calibrated by setting the peak of pore size distribution for the largest diameter to coincide with the manufacturer's supplied nominal pore size, and arrows mark the average pore sizes supplied by the manufacturer for the other two samples. For clarity, distributions for glasses with 15.6 and 23.7 nm nominal pore diameters are shifted vertically.

It is well-known that at temperatures below the melting point of a material imbibed in pores there exists a layer of liquidlike material confined between the frozen bulk of pore liquid and the pore wall.[22,23] The exact extension of this layer as defined by diverse techniques is still a matter of controversy. In the case of water and oxide surfaces, calorimetric[24] or NMR[13,25] studies put the width of this layer in the range of 1−3 water monolayers. Since K is a substance property and thereby independent of pore size, we can estimate the importance and effect of this surface layer on pore size determination by investigating CPGs with different pore sizes. In Figure 3 we show the pore size distributions for three different nominal (measured by mercury intrusion and given as supplied by the manufacturer) pore diameters. Clearly, the average pore sizes measured by NMR cryoporometry and mercury intrusion coincide well, which indicates a surface layer of our salt hydrate of <1 nm width. This estimate is further supported by the temperature dependence of the transverse relaxation time T_2; at temperatures below the melting point of pore liquid there is a small (in the order of a percent) signal contribution with a short (~1 ms) T_2 value. Because of its short T_2, this signal, which plausibly originates from the nonfreezing surface layer, is suppressed in the spin−echo detection of $I(T)$. Finally, we note that the coincidence of average pore sizes by NMR cryoporometry and mercury porosimetry also indicates that the variation of relevant substance properties (such as ΔH_f) by pore size is small.

Conclusions

The pore size distributions for controlled pore glasses have been obtained by ^{1}H NMR cryoporometry via observation of the melting of a pore-confined transition-metal salt hydrate, $Zn(NO_3)_2 \cdot 6H_2O$. The melting point shift of this material proves to be more than twice as large as that for water. Hence, this and similar inorganic salt hydrates can be sensitive probes of pore sizes and size distributions.

Although we have data for volume expansion upon melting in only a few salt hydrates,[26] those values are all positive (e.g., 5.3% for $Mg(NO_3)_2 \cdot 6H_2O$). Hence, salt hydrates seem to expand upon melting and contract upon freezing, which is opposite the behavior of water. This feature might turn out to be advanta-

geous in hydrophilic porous systems such as cellulose-based ones,[27] where the volume expansion of water upon freezing might modify the porous structure (as demonstrated in other systems[28]) that one intends to study.

One should also note that such salt hydrates have rather large enthalpies of fusion (see Table 1), too; this is the underlying reason for their application as thermal energy storage materials.[14] Hence, they are also well-suited for thermoporometric experiments where pore sizes and size distributions are derived from DSC observations of freezing−melting.

Acknowledgment. This work has been supported by the Swedish Science Council (VR). D.V.F. thanks Conacyt, Mexico, for a scholarship. O.P. thanks Carl Tryggers Stiftelse for a scholarship.

References and Notes

(1) Jackson, C. L.; McKenna, G. B. *J. Chem. Phys.* **1990**, *93*, 9002−9011.
(2) Ishikiriyama, K.; Todoki, M. *J. Colloid Interface Sci.* **1995**, *174*, 103−111.
(3) Ishikiriyama, K.; Todoki, M.; Motomura, K. *J. Colloid Interface Sci.* **1995**, *171*, 92−102.
(4) Overloop, K.; Van Gerven, L. *J. Magn. Reson. A* **1993**, *101*, 179−187.
(5) Strange, J. H.; Rahman, M.; Smith, E. G. *Phys. Rev. Lett.* **1993**, *71*, 3589−3591.
(6) Hansen, E. W.; Schmidt, R.; Stöcker, M. *J. Phys. Chem.* **1996**, *100*, 11396−11401.
(7) Hansen, E. W.; Simon, C.; Haugsrud, R.; Raeder, H.; Bredesen, R. *J. Phys. Chem. B* **2002**, *106*, 12396−12406.
(8) Valiullin, R.; Furó, I. *J. Chem. Phys.* **2002**, *116*, 1072−1076.
(9) Christenson, H. K. *J. Phys. Condens. Matter* **2001**, *13*, R95−R133.
(10) Denoyel, R.; Pellenq, R. J. M. *Langmuir* **2002**, *18*, 2710−2716.
(11) Petrov, O.; Furó, I. *Phys. Rev. E* **2006**, *73*, in press.
(12) Valiullin, R.; Furó, I. *Phys. Rev. E* **2002**, *66*, 031508.
(13) Valiullin, R.; Furó, I. *J. Chem. Phys.* **2002**, *117*, 2307−2316.
(14) Farid, M. M.; Khudhair, A. M.; Razack, S. A. K.; Al-Hallaj, S. *Energy Convers. Manage.* **2004**, *45*.
(15) Jain, S. K. *J. Chem. Eng. Data* **1978**, *23*, 170−173.
(16) Ewing, W. W. *J. Am. Chem. Soc.* **1939**, *61*, 260−265.
(17) Ansell, S.; Neilson, G. W. *Biophys. Chem.* **2004**, *107*, 229−241.
(18) Ferrari, A.; Braibanti, A.; Manotti-Lanfredi, A. M.; Tiripicchio, A. *Acta Crystallogr.* **1967**, *22*, 240−246.
(19) Yuvaray, S.; Lin, F. Y.; Chang, T. H.; Yeh, C. T. *J. Phys. Chem. B* **2003**, *107*, 1044−1047.
(20) Wahab, A.; Mahiuddin, S. *J. Chem. Eng. Data* **2004**, *49*, 126−132.
(21) Aksnes, D. W.; Forland, K. *Appl. Magn. Reson.* **2003**, *25*, 297−311.
(22) Dash, J. G. *Rev. Mod. Phys.* **1999**, *71*, 1737−1743.
(23) Dash, J. G.; Fu, H.; Wettlaufer, J. S. *Rep. Prog. Phys.* **1995**, *58*, 115−167.
(24) Ishizaki, T.; Maruyama, M.; Furukawa, Y.; Dash, J. G. *J. Cryst. Growth* **1996**, *163*, 455−460.
(25) Xie, X. L.; Satozawa, M.; Kunimori, K.; Hayashi, S. *Microporous Mesoporous Mater.* **2000**, *39*, 25−35.
(26) Minevich, A.; Marcus, Y.; Ben-Dor, L. *J. Chem. Eng. Data* **2004**, *49*, 1451−1455.
(27) Furó, I.; Daicic, J. *Nord. Pulp Pap. Res. J.* **1999**, *14*, 221−225.
(28) Allen, S. G.; Stephenson, P. C. L.; Strange, J. H. *J. Chem. Phys.* **1998**, *108*, 8195−8198.
(29) Kiselev, S. B. *Int. J. Thermophys.* **2001**, *22*, 1421−1433.
(30) Riesenfeld, E. H.; Milchsack, C. *Z. Anorg. Chem.* **1914**, *85*, 401−429.
(31) Perry, J. H. *Chemical Engineers' Handbook*, 7th ed.; McGraw-Hill: New York, 1997.
(32) Angell, C. A.; Tucker, J. C. *J. Phys. Chem.* **1974**, *78*, 278−281.
(33) Guion, J.; Sauzade, J. D.; Lauegt, M. *Thermochim. Acta* **1983**, *67*, 167−180.
(34) Meisingset, K. K.; Gronvold, F. *J. Chem. Thermodyn.* **1983**, *18*, 159−173.
(35) Shomate, C. H.; Young, F. E. *J. Am. Chem. Soc.* **1944**, *66*, 771−773.